Ritchie H, Jamieson AJ, Piertney SB.

Population genetic structure of two congeneric deep-sea amphipod species from geographically isolated hadal trenches in the Pacific Ocean.

***Deep-Sea Research Part 1* 2017, 119, 50-57**

Population genetic structure of two congeneric deep-sea amphipod species from geographically isolated hadal trenches in the Pacific Ocean

Authors: Ritchie, H.[a], Jamieson, A.J.[b*], and Piertney, S.B.[a]

[a] Institute of Biological and Environmental Sciences, University of Aberdeen, Zoology Building, Aberdeen AB24 2TZ, UK

[b] Oceanlab, University of Aberdeen, Newburgh, Aberdeenshire AB41 6AA, UK

*Present Address: School of Marine Science and Technology, Ridley Building, Newcastle University, Newcastle Upon Tyne, UK NE1 7RU

Corresponding Author: Ritchie, H.[a] email: heather.ritchie.07@aberdeen.ac.uk

Abstract

The deep ocean trenches that comprise the hadal zone have traditionally been perceived as a series of geographically isolated and demographically independent features likely to promote local species endemism through potent natural selection and restricted dispersal. Here we provide the first descriptions of intraspecific population genetic structure among trenches from which the levels of genetic connectivity can be examined explicitly. A total of 109 individuals across two species of *Paralicella* amphipods (Lysianassoidea: Alicellidae) were genotyped at 16 microsatellite DNA loci. An analysis of molecular variance identified that 22% of the overall genetic variance was attributable to differences between the species and a further 7% was attributable to differences between populations. The two species showed different patterns of genetic structure, with the levels of genetic differentiation between trenches explained by geographical proximity, the geological ages of the trenches, contemporary bottom current patterns and seabed topography around the Pacific Ocean. Overall, the inferred levels of gene flow among trenches was sufficient to reject the hypothesis that they are evolutionarily independent units.

Keywords: Hadal trenches; Amphipoda; deep sea ecology; connectivity; gene flow; endemism

Highlights

- Hadal trenches do not represent demographically independent entities in *Paralicella*
- Patterns of connectivity between trenches differ for two *Paralicella* species
- Trench geological ages, deep water currents and topography explain connectivity

1. Introduction

The hadal zone is the deepest marine biome, extending from 6000 m to full ocean depth at approximately 11,000 m at the Challenger Deep in the Mariana Trench. It is primarily comprised of 37 trench systems which are formed along subduction zones between tectonic plates, with the majority located around the Pacific Rim (Jamieson et al., 2010). Trenches break the continuum of the abyssal plains by forming disjunct clusters of ultra-deep habitat "islands". The hadal zone accounts for over 45% of the total vertical depth of the marine environment (Jamieson 2015) and it is characterised by high hydrostatic pressure, cold temperatures, low food availability and an absence of natural light (Wolff, 1960). Despite being considered an "extreme" environment the hadal zone is host to a diverse range of flora and fauna, notably the Isopoda, Polychaeta, Gastropoda and Amphipoda (Wolff, 1970, Belyaev, 1989).

The restricted distribution of key taxa within these groups to specific trenches underpins the conventional view that hadal trenches are hotspots of species endemism driven by a combination of geographic isolation and potent selection pressures (Wolff 1960; Wolff 1970). For example, within the amphipod genus *Hirondellea*, *H. dubia* is restricted to the Kermadec, Tonga and New Hebrides trenches in the southwest Pacific (Lacey et al., 2016), *H. gigas* is located in all studied trenches of the northwest Pacific (France 1993), and newly described *Hirondellea* species have been identified in the Peru-Chile Trench in the southeast Pacific (Fujii et al., 2013; Kilgallen 2015). However, this assertion that hadal trenches are hotspots of species endemism is difficult to reconcile with the seemingly cosmopolitan distribution of other amphipod species. For example, *Eurythenes gryllus* which has been described as having a pan-oceanic distribution from bathyal to hadal depths, and has been

located in every hadal trench investigated to date in addition to the intervening abyssal plains (Barnard, 1961; Thurston et al., 2002; Havermans et al., 2013; Eustace et al., 2016). This cosmopolitan distribution of a supposedly single *E. gryllus* species is complicated by morphological and phylogeographic differences between different populations (Havermans et al., 2013) and even within a single trench population (Eustace et al., 2016). This suggests *E. gryllus* may actually represent multiple species each defined by geographic and bathymetric isolation and associated drift and selection (Havermans, 2016).

A capacity for hadal trenches to promote genetic divergence within and between species appears counter to the depth-differentiation hypothesis (Rex and Etter, 2010). This states there should be a reduction in barriers to gene flow with increasing depth from the continental shelf due to the increase in environmental homogeneity with bathymetric depth. A growing body of data from across deep-sea environments in the bathyal and abyssal zones supports the depth-differentiation hypothesis, largely showing connectivity between populations (e.g. Cowart et al., 2004; Quattrini et al., 2015; Ritchie et al., 2013). It is unclear how disjunct topographical features such as seamounts, spreading centres (ridges), fracture zones and canyons disrupt the depth differentiation paradigm, but it appears patterns of genetic structure are variable across taxa, life history strategies and geographic locations (Baco et al., 2016; Clark et al., 2010). To date there has been no indication of how the hadal zone fits into the depth-differentiation hypothesis paradigm, primarily because of the dearth of information on population genetic structure based upon the distribution of neutral genetic variation. A demonstration that hadal trenches have equivalent frequencies of neutral polymorphisms would indicate a high degree of connectivity, and conversely significant genetic structure would highlight that each trench represents a demographically independent unit with minimal gene flow. Examining the patterns of gene flow in the context of trench location, geological ages of trenches, topographical features of the abyssal plains and contemporary bottom currents will allow speculation on possible routes of historical colonisation of the hadal trenches and identify the major drivers influencing patterns of dispersal at an oceanic scale.

Here we examine the patterns of genetic structure between populations from across five hadal trenches around the Pacific Rim for two putative species of the Lysianassoid genus *Paralicella*. These two sister species provide an excellent model for testing patterns of gene flow as they have an abyssal-hadal distribution (Barnard and Schulenberger, 1976; De Broyer et al., 2004) allowing us to examine differences between trenches in the context of dispersal patterns across the intervening abyssal plains. They also have overlapping pan-oceanic geographical distributions (Barnard and Shulenberger, 1976; Thurston, 1979) that will facilitate examination of parallel patterns of connectivity across trench populations across the species.

This study represents the first investigation elucidating patterns of gene flow and connectivity between hadal trenches. We exploit a suite of microsatellite DNA markers that were previously mined from an Illumina MiSeq library of *P. tenuipes* (Ritchie et al., 2016) to test the null hypothesis that there is extensive gene flow between trench populations, in both species, leading to a lack of significant population genetic structure.

2. Materials and Methods

2.1 Sample collection

A total of 109 amphipods were collected from across five hadal trenches over the course of six sampling campaigns between 2007 - 2013 using an autonomous deep-ocean lander vehicle (Jamieson et al., 2009) incorporating small baited funnel traps (see Table 1 and Ritchie et al., 2015). Upon recovery of the lander, amphipods were transferred immediately to 99% ethanol prior to morphological identification to genus level in a shore-based laboratory (National Institute for Water and Atmospheric Research, New Zealand or latterly the Australian Museum) using morphological characteristics outlined in Barnard and Karaman (1991). Total genomic DNA was extracted from the whole body of individual specimens using a standard phenol-chloroform approach.

2.2 Species identification

The *Paralicella* genus has traditionally been considered to contain two predominant species, *P. tenuipes* and *caperesca* (Barnard and Schulenberger, 1976). According to their taxonomic descriptions *P. tenuipes* is distinguished from *P. caperesca* as it has a heavily bevelled article 2 on pereopod 5 and a non-bevelled coxa 1 whereas *P. caperesca* has a non-bevelled pereopod 5 and a bevelled coxa 1 (Barnard and Shulenberger, 1976). However, identification of these *Paralicella* species has been problematic given the minute differences in morphological characters used to differentiate between them. This is further confused by ontogenetic variation and phenotypic plasticity which has been shown for these two species (Barnard and Shulenberger, 1976). Recent molecular phylogenetic analysis based upon mitochondrial 16S and COI markers (Ritchie et al., 2015) identified two distinct phylogenetic clades within the *Paralicella* genus consistent with the presence of two species, but these were not congruent with the morphological characteristics conventionally used to distinguish *P. caperesca* and *P. tenuipes*. As such, here we define species within the *Paralicella* genus from their diagnostic mitochondrial DNA COI sequences using a standard restriction fragment length polymorphism (RFLP) assay. A 710bp fragment of the COI locus was PCR amplified using the COI primers and conditions outlined in Ritchie et al., (2015). PCR amplicons were then double-digested for 2 hours at 37°C with 1.5 units of each of the restriction enzymes *Mbo*II and *Nla*III. Restriction profiles were visualised using agarose electrophoresis with individuals producing a two-band profile (135bp and 575bp) being classified as RFLP sp. 1 (Group 1 in Ritchie et al., 2015) and individuals with a three-band profile (135bp, 220bp and 355bp) being classified as RFLP sp. 2 (Groups 2, 3 and 4 in Ritchie et al., 2015).

In total, the 109 individuals were separated into seven *a priori* populations of *Paralicella* spp. RFLP sp. 1 individuals were found in the Kermadec (n=4), Japan (n=24), Mariana (n=24) and Peru-Chile trenches (n=15), and RFLP sp. 2 individuals were found in the Kermadec (n=26), Peru-Chile (n=2) and New Hebrides trenches (n=14).

2.3 Microsatellite genotyping

All individuals were genotyped at 16 microsatellite loci designed specifically for *Paralicella* (Ritchie et al., 2016). PCR reaction conditions followed Ritchie et al., (2016) and amplicons were resolved using an ABI 3730 DNA Capillary DNA Sequencer (Dundee, DNA Sequencing Services Ltd). Genotypes were scored by eye with Genemarker v 1.4 (SoftGenetics, 2010) against a GD-500 (LIZ) size standard.

Deep sea samples often yield poor quality DNA due to both the extreme change in hydrostatic pressure that results in cell and DNA damage (Dixon et al., 2004), and the DNA degradation that ensues given the by time between collection and preservation (Hofeiter et al., 2001). This can lead to

loss of individual genotypes across samples, and as such here we based analysis on samples that yielded over 80% amplification success, and through trial analysis using jack-knifed datasets confirmed that interpretation was robust to the overall genotyping success rate.

2.4 Population genetic analyses

Micro-Checker 2.2.3 (van Oosterhout et al., 2004) was used to establish whether any heterozygote deficiencies were attributable to null alleles and/or scoring errors. Linkage disequilibrium between all combinations of loci for each sampling location was tested using Genepop 4.0.10 (Raymond and Rousset, 1995; Rousset, 2008) and significance was evaluated using Fisher's exact test with Bonferroni correction (Ryman et al., 2006). Genetic diversity was described using observed heterozygosity (H_O), number of effect alleles (n_e) and allelic richness (a_r) in the diveRsity package in R (Keenan et al., 2013).

To estimate the proportion of genetic differentiation attributable to differences between the RFLP defined species and between populations of the same species but from different trenches, a hierarchical analysis of molecular variance (AMOVA) was implemented using GenAlEx 6.5 (Peakall and Smouse, 2006).

Structure 2.3.3 (Pritchard et al., 2000) was used to implement Bayesian MCMC inference of *a posteriori* genetic clusters across the entire dataset combined and within the RFLP-defined species. The number of assumed genetic clusters (K) was set from one to seven, with 10 independent runs performed for each value of K. A total of 10,000,000 MCMC iterations were run using the admixture ancestry model with correlated allele frequencies where the first 100,000 iterations were discarded as burn-in. Analyses were run both with and without sampling location as prior information for the model (*loc prior)*. Structure Harvester 0.6.7 was used to collate the results and infer the statistically best supported K using both the maximum log likelihood (Pritchard et al., 2000) and the ΔK statistic (Evanno et al., 2005). Replicate runs for each K were then aligned and averaged in Clumpp 1.1.2 (Jakobsson and Rosenberg, 2007) using the Greedy algorithm with 10 randomised input orders, and visualised using Distruct 1.1 (Rosenberg, 2004).

Population structure was also resolved using a model-free multivariate ordination approach of discriminant analysis of principal components (DAPC) implemented in the *adegenet* package in R (Jombart, 2008). All principal components were included into the k-means clustering algorithm from K_{DAPC}=1 to K_{DAPC}=7, and the optimal K_{DAPC} was selected using the Bayesian information criterion. A total of 20 principal components were retained for the discriminant analysis, though changing the number of principal components did not affect the output. All discriminant functions were retained. A second DAPC analysis was run using the seven *a priori* populations to explore the genetic differentiation among these populations.

Pairwise genetic differentiation was estimated using F_{ST} (Weir and Cockerham, 1984) for populations where sample size was over 24 and thus amenable to frequency-based comparison. Values were calculated using diveRsity and significance was evaluated using Fisher's exact test with Bonferroni correction.

Pairwise F_{ST} was correlated against Euclidian geographic distances estimates for both RFLP sp. 1 and RFLP sp. 2 to test for an isolation-by-distance effect using IBD 3.23 (Bohonak, 2002). Significance was assessed using a Mantel test (10,000 randomisations).

Migrate-n (Beerli, 2008) was used to infer migration patterns and rates among the *a priori* populations of the two genetically defined species. The population mutation rate parameter θ ($\vartheta=4N_e\mu$, where N_e is the effective population size and μ is the mutation rate per site) and the migration rate, M ($M=m/\mu$, where m is the immigration rate per generation) were estimated both by maximum likelihood and Bayesian methods, using a coalescent approach. Two replicates were performed for all population groups to check for convergence of parameter estimates. For the analysis the Brownian mutation model was used, the relative mutation rate was estimated from the data, and a random tree were used as a start point. A matrix of geographical distances between the trenches was also included so that the migration rate is not only scaled by the mutation rate but also by the distance matrix in order to detect environmental barriers. The Bayesian analysis was run for 10 short and two long chains with 100,000 recorded genealogies where the first 10,000 genealogies were discarded as burn-in.

Migrate-N was also used to compare among three models of connectivity between the populations that best explain the distribution of genetic diversity in each clade: 1) a "full" model with symmetrical migration between all populations; 2) a "current" migration model that follows the directional movements of the deep water currents shown in Figure 3; and, 3) a "counter-current" model that assumes opposite current directions from the "current" model. The best fit model was identified by comparing the computed Bezier marginal likelihood and Bayes factor scores.

The function divMigrate from the diveRsity package in R (Keenan et al., 2013) was also used to calculate direction-relative migration using Jost's D as a measure of genetic distance and 10,000 bootstraps replications were performed to test for statistical significance.

3. Results

3.1 Diversity Statistics

Tests for linkage disequilibrium identified no significant interactions ($p>0.05$, Fisher's exact test) between any of the pairwise comparisons indicating that none of the loci are physically linked. Micro-checker did not highlight any incidences of either null alleles or scoring errors.

Diversity statistics calculated by diveRsity are presented in Table 2. Across all populations the allelic richness ranged from 0.66 to 3.68 with an average of 2.67. Allelic richness was similar between the two species with RFLP sp. 1 allelic richness ranging from 1.81 to 3.47 with an average of 2.96, and RFLP sp. 2 allelic richness ranging from 0.66 to 3.68 with an average of 2.97. Observed (H_O) heterozygosities ranged from 0.21 to 0.38 across all populations. For RFLP sp. 1 H_O ranged from 0.18 to 0.38, and RFLP sp. 2 H_O ranged from 0.03 to 0.22. The low values of allelic richness and observed heterozygosity for the RFLP sp. 1 Kermadec population and the RFLP sp. 2 Peru-Chile population are attributable to their small sample sizes.

3.2 Genetic differentiation

The AMOVA analysis identified that 21% of the overall variance was attributable to differences between the RFLP-identified species ($p<0.001$) and that 7% of the variance was attributable to differences between the seven *a priori* populations within the two species ($p<0.001$) (Table 4). As such, the variance between species was three times higher than between populations. The remaining variance was accounted for by differences among individuals within populations ($p<0.001$).

Bayesian clustering analysis conducted in Structure indicated that the best supported number of posterior genetic clusters was K=2 using both the maximum log likelihood and the ΔK criteria. Under this model individuals were partitioned correctly into their RFLP-defined species. Structure analysis within RFLP-sp. 2 separated New Hebrides Trench samples from the Kermadec and Peru-Chile Trench samples (Figure 1b). There was no further partitioning of RFLP-sp. 1 samples into different trenches (Figure 1a). This lack of structure within RFLP-sp. 1 belies estimates of population genetic structure inferred from Weir and Cockerham's (1984) F_{ST} where pairwise comparison between Japan and Mariana, Mariana and Peru-Chile, and Peru-Chile and Japan were all significantly different from zero after Bonferroni correction (F_{ST} estimates of 0.02, 0.05 and 0.05, respectively).

The patterns of differentiation from the Structure analysis are congruent with that from a multivariate ordination in DAPC. The discriminant functions obtained from the DAPC analysis were plotted in a distribution plot for $K_{DAPC}=2$ and an ordination plot for $K_{DAPC}=3$ (Figure 2a and b, respectively). With $K_{DAPC}=2$ there is a strong separation into the two genetically distinct species where the majority of the differentiation is explained by the first discriminant function. With $K_{DAPC}=3$ there is clear hierarchical structure both between the two species and also between the populations belonging to RFLP sp. 2. Differentiation is maintained between RFLP sp. 1 and RFLP sp. 2 by the first discriminant function and the differentiation between the RFLP sp. 2 New Hebrides population and the Kermadec and Peru-Chile trench populations is differentiated by the second discriminant function.

Whilst there is a trend towards increasing genetic distance with geographic separation between trenches, this was insignficant for both RFLP sp. 1 and RFLP sp. 2 ($p=0.32$ and 0.33 respectively.

3.3 Migration patterns

Migrate-n calculated the number of immigrants per generation (ΘM) which are shown in full (Table 5) and summarised visually (Figure 3). These results indicate Pan-Pacific migration between different trench populations for RFLP sp. 1 and that migration is considerably less for populations in RFLP sp. 2. For RFLP species 1 migration estimates suggest that individuals from Japan, Mariana, Kermadec and Peru-Chile trenches all migrate reciprocally, with the exception of no migration between the Kermadec Trench and Japan Trench. Migration was highest between the Japan and Mariana trenches which is likely to be attributed to their geographic proximity. In both instances migration from the Peru-Chile Trench to the Japan and Mariana trenches was greater than from the Japan and Mariana trenches to the Peru-Chile Trench. Furthermore, migration between the Peru-Chile Trench and the Kermadec Trench was considerably lower in both directions. All migration into the Kermadec Trench is considerably low overall and lower than the migration out of the Kermadec Trench in all instances. For RFLP sp. 2 the analysis again suggested some migration from the Peru-Chile Trench to Kermadec but with no reciprocal migration. The analysis also highlighted the apparent isolation of

the New Hebrides Trench where there is no migration either into or out of the trench from either the Kermadec or Peru-Chile trench.

Migrate-n also identified that for RFLP sp. 1the distribution of genetic diversity was best explained by a model that followed the patterns of deep ocean currents. However for RFLP sp.2, the optimal model followed the "full" island model with symmetrical gene flow, through the likelihood of this model was close to that of the "current" model (Supplementary table 1).

The divMigration method provided similar results to the Migrate-n analyses with the exception that it suggested some bidirectional migration between the RFLP sp. 2 Kermadec and Peru-Chile trenches, but this was not statistically significant. Migration between the Kermadec and Peru-Chile trenches is difficult to determine absolutely due to the small Peru-Chile population size (n=2) which particularly affects the divMigration analysis due to its use of Jost's D.

4. Discussion

The salient finding of this study is that there is a level of population genetic structure between trenches for both of the *Paralicella* amphipod species that is sufficient to indicate the trenches do not form a single panmictic population, but insufficient to designate that hadal trenches as demographically independent units. This finding is counter to the traditionally perceived view point that trenches represent geographically and genetically isolated habitats that promote high levels of species endemism. The levels of genetic structure observed are indicative of some degree of gene flow and connectivity between the trenches for *Paralicella* amphipods, even over large geographical scales.

There was clear and obvious differentiation between the two RFLP-identified species. From the analysis of molecular variance this separation accounted for 21% of the overall variance observed. This high level is not surprising given these two groups represent individual species with a high level of mitochondrial DNA sequence divergence (Ritchie et al., 2015). The debate remains about whether these RFLP species reflect the morphological forms that define *P. caperesca* and *P. tenuipes* descriptions. Clearly a much more dove-tailed comparison of morphological and genetic data for *Paralicella* spp. needs to be undertaken, but that is beyond the scope of the current study. Irrespective of whether they represent the two previously described species it is clear that two species do exist.

Within each of the two species there was a signature of population genetic structure. The AMOVA indicated that differences between populations within the RFLP species accounted for 7% of the overall variance. The two RFLP species did differ overall in their patterns of population genetic structure.

For RFLP sp. 1 the Structure and DAPC based analyses could not discern between the Kermadec, Japan, Peru-Chile and Mariana samples, though frequentist analysis via pair-wise F_{ST} did identify significant levels of differentiation. Structure is known to return false-negatives when population structure is minor (below 5%; Latch et al., 2006), but the sample sizes certainly between Japan and Mariana are sufficient to suggest that the significant F_{ST} estimates are not artefacts and do reflect true structure. Moreover, the F_{ST} estimates between Japan and Mariana are smaller than between either of these populations and the Peru-Chile trench, consistent with their proximity.

For RFLP sp. 2 a more pronounced genetic structure was resolved. For both the Structure and DAPC analyses the Kermadec and Peru-Chile trenches were separated from the New Hebrides trench.

The patterns of genetic structure for the two RFLP species can be explained by a combination of geological ages of the trenches, contemporary bottom current patterns, and seabed topography around the Pacific Ocean. The geological ages of the trenches goes some way to explaining the distributions of the two RFLP species. The two oldest trenches investigated here are the Mariana and Kermadec trenches, which were formed approximately 150 MYA and 120 MYA, respectively (Stern, 2002). As the oldest trenches in the Pacific Ocean they will have been colonised by a common ancestor of the modern *Paralicella* genus and the geographic distance between the trenches may have led to the isolation and subsequent speciation into the two RFLP species. Once established as two separate species they will both have been able to colonise new trenches as they formed. Individuals of RFLP sp. 1 would be more likely to colonise the Japan Trench from the Mariana Trench given their geographical proximity. Likewise, individuals of RFLP sp. 2 will have been able to migrate from the Kermadec to the New Hebrides Trench. The Peru-Chile Trench is one of the geologically youngest Pacific trenches as it was only formed approximately 40 MYA (Stern, 2002). It is the most remote trench from the Kermadec and Mariana trenches but is approximately equidistance from them potentially allowing it to be colonised by both RFLP species.

Contemporary bottom current patterns provide an explanation for ongoing dispersal among trenches for both RFLP species. Reid (1997) documented a large water mass that flows from the East to West Pacific Ocean around the equator which could have the potential to enable individuals of both species to migrate from the Peru-Chile Trench to the Kermadec Trench across the abyssal plains. Reciprocal migration of RFLP sp. 1 individuals between the Japan and Peru-Chile trenches can also be explained by a North-Western current moving away from the Peru-Chile Trench (Shaffer et al., 1995) and a South-Eastern current moving away from the Japan Trench (Mitsuzawa, 1998). Notwithstanding, there is no current data available for the intervening regions between the Japan and Peru-Chile trenches and furthermore it is unclear how abyssal topography will affect either of these currents between them, and certainly it has been noted that bottom water masses near the Japan Trench are disturbed and redistributed due to fine-scale interactions with large topographical features, particularly the Kuril-Kamchatka and Aleutian trenches (Mitsuzawa, 1998; Kawabe and Fujio, 2003, 2010). The interaction of currents with topographical features is particular pertinent to note when considering current movement around the Kermadec Trench, where the Kermadec forearc breaks and disrupts currents and gyres (Reid, 1986). This may go some way towards explaining why migration in and out of the Kermadec Trench is comparatively lower than other trenches. Some of the patterns of migration inferred from the genetic data are more difficult to reconcile. For example, it is unclear why there is reciprocal migration between the Mariana and Kermadec trenches but not between the Japan and Kermadec trenches given the proximity of the Japan and Mariana trenches. Such patterns may be better explained once more detailed data on localised deep-water hydrography from the area are available.

It also appears difficult to explain how there are significant differences between RFLP species 2 populations in the Kermadec and New Hebrides trenches given their overall proximity. This could be explained by a combination of topographical features and bottom current flow. Geologically the New Hebrides Trench was connected to the Tonga and Kermadec trenches due to the overlap between the Australian and Pacific tectonic plates (Pellentier et al., 1998) up to around 30 MYA in

the Oligocene (Schellart et al., 2002). Their subsequent separation could have isolated individuals between the New Hebrides and Kermadec trenches. The current lack of migration between the two populations may be attributed to the Tonga-Kermadec forearc which is a topographical feature that rises to between ~1000 m to ~2000m depth creating a physical barrier that prevents dispersal (Karig, 1970). The Kermadec forearc is, however, considered a "leaky barrier" as the frontal ridge flattens to a bench at abyssal depths between 3500 m and 5000 m which is sufficiently deep to allow individuals to migrate across it (Karig, 1970b). If individuals are able to cross the forearc they will enter a separate gyre-within-a-gyre current system that has formed from interactions between the deep Antarctic Circumpolar Current and the East Australia Current between Australia, New Zealand and the Tonga-Kermadec forearc (Davis, 1998) which may prevent migration from the New Hebrides Trench to the remainder of the Pacific Ocean.

The differences in distribution between RFLP sp. 1 and sp. 2 make a direct comparison of patterns of dispersal between the two species difficult. The only direct comparison can be made is between the Kermadec and Peru-Chile trenches. In this case the patterns of population structure are different between the two species where RFLP sp. 1 shows a bidirectional migration patterns and RFLP sp. 2 shows a unidirectional migration pattern. However, whether this reflects a true biological difference in dispersal rates or propensity, or if it is merely a consequence of low sample size in RFLP sp. 2 in the Peru-Chile Trench is debatable. There is extremely little known about life history parameters in the *Paralicella* genus to point to any differences between species that could explain the differences in population genetic structure across these two species.

Indeed, a lack of understanding of fundamental life history parameters in *Paralicella* makes it difficult to explain the mechanism through which gene flow is most readily facilitated over large geographical distances between trenches. It is known that *Paralicella*, in line with the majority of deep sea scavenging amphipods, does not have a larval dispersal phase (Dolah and Bird, 1980) that would promote dispersal over large distances within the plankton. This would therefore point to dispersal and gene flow being mediated through either the movement of juveniles or adults. In other species of hadal amphipods there is clear ontogenetic structure, with juveniles occurring at shallower depths (Eustace et al., 2016) which may predict that the juvenile phase is more likely to disperse. Moreover, given *Paralicella* has a distribution that encompasses both hadal and abyssal zones it is easier to envisage direct linkages between different trenches mediated via stepping stone dispersal across the abyssal plains and an overall pattern of isolation-by-distance. However, a challenge moving forward is to elucidate the mechanisms of dispersal and gene flow in this genus and compare the patterns of population genetic structure with amphipod species that have a restricted hadal distribution.

Our data clearly demonstrate that for *Paralicella* amphipods, the hadal trenches are not effectively isolated habitats, but that some cross-talk via gene flow is possible. The challenge moving forward is determining how general this picture is across the Amphipoda, and a broader taxonomic range of hadal and abyssal taxa. The patterns of genetic structure resolved here, coupled with what is already known about species distribution within (Eustace et al., 2016) and between trenches (Lacey et al., 2016) suggests that hadal trenches lie somewhere between the ends of a continuum bounded by the basic premise of oceanic panmixia predicted by the depth-differentiation hypothesis, and the traditional perspective of trenches as evolutionarily and demographically independent units. For

each species, the position on this continuum will be defined by life history and local oceanography, as appears to be the case for hydrothermal vent and seamount communities.

Acknowledgements

This work was supported by the HADEEP projects, funded by the Nippon Foundation, Japan (2009765188), the Natural Environmental Research Council, UK (NE/E007171/1) and the Total Foundation, France. We acknowledge additional support from the Marine Alliance for Science and Technology for Scotland (MASTS) funded by the Scottish Funding Council (Ref: HR09011) and the Leverhulme Trust (to SBP). Additional sea time was supported by NIWA's 'Impact of Resource Use on Vulnerable Deep-Sea Communities' project (CO1_0906). We thank the chief scientists, crew and company of the Japanese RV *Hakuho-Maru* (KH0703 and KH0803), the RV *Tansei-Maru* (KT-09-03), the RV *Kairei* (KR0716), the German FS *Sonne* (SO197 and SO 209) and the New Zealand RV *Kaharoa* (KAH0190, KAH1109, KAH1202, KAH1301 and KAH1310). From NIWA, we thank Malcolm Clark, Ashley Rowden, Kareen Schnabel, Sadie Mills for logistical support at the NIWA Invertebrate Collection. We also thank Marius Wenzel for helpful comments on manuscript drafts, and Dr. Tammy Horton (NOCS, UK) and Naimh Kilgallen (Australian Museum, Sydney) for identification of amphipod samples.

392 **References**

393 Baco, A., Etter, R., Ribeiro, P., von der Heyden, S., Beerli, P., & Kinlan, B. P. (2016). A
394 synthesis of genetic connectivity in deep-sea fauna and implications for marine reserve
395 design. *Molecular Ecology*. doi.org/10.1111/mec.13689

396 Barnard, J., & Karaman, G. S. (1969). The families and genera of marine gammaridean
397 Amphipoda. Part 2. *Rec. Austr. Mus. Suppl.*, *13*, 1–417 419–866.

398 Barnard, J. L. (1961). Gammaridean Amphipoda from depths of 400 to 6000 meters.
399 *Galathea Report*, *5*, 23–128.

400 Barnard, J. L., & Shulenberger, E. (1969). The families and genera of marine Gammaridean
401 Amphipoda. Part 1. *Crustaceana*, *31*(4), 267–274.

402 Beerli, P. MIGRATE-N: estimation of population sizes and gene flow using the coalescent.
403 *Avaliable from popgen.scs.fsu.edu/Migrate-N.html*.

404 Beliaev, G. (1989). Deep sea ocean trenches and their fauna. *Nauka, Moscow*.

405 Bohonak, A.J., 2002. IBD (Isolation by Distance): A program for analyses of isolation by
406 distance. J. Hered. 93, 153–154. doi:10.1093/jhered/93.2.153

407 Broyer, C. De, Nyssen, F., & Dauby, P. (2004). The crustacean scavenger guild in Antarctic
408 shelf, bathyal and abyssal communities. *Deep Sea Research Part II: Topical Studies in*
409 *Oceanography*, *51*(14-16), 1733–1752.

410 Clark, M., Rowden, A., Schlacher, T., Williams, A., Consalvey, M., Stocks, K. I., Hall-Spencer, J.
411 M. (2010). The ecology of seamounts: structure, function, and human impacts. *Annual*
412 *Review of Marine Science*, *2*, 253–278.

413 Cockerham, C., & Weir, B. (1984). Covariances of relatives stemming from a population
414 undergoing mixed self and random mating. *Biometrics*, *40*(1), 157–164.

415 Cowart, D., Halanych, K., Schaeffer, S., & Fisher, C. (2014). Depth-dependent gene flow in
416 Gulf of Mexico cold seep Lamellibrachia tubeworms (Annelida, Siboglinidae).
417 *Hydrobiologia*, *736*(1), 139–154.

418 Davis, R. (1998). Preliminary results from directly measuring middepth circulation in the
419 tropical and South Pacific. *Journal of Geophysical Research: Oceans*, *103*, 24619–24639.

420 Dixon, D., Pruski, A., & Dixon, L. (2004). The effects of hydrostatic pressure change on DNA
421 integrity in the hydrothermal-vent mussel Bathymodiolus azoricus: implications for
422 future deep-sea. *Mutation Research/Fundamental and Molecular Mechanisms of*
423 *Mutagenesis*, *552*(1-2), 235–246.

424 Dolah, R. F. Van, & Bird, E. (1980). A comparison of reproductive patterns in epifaunal and
425 infaunal Gammaridean amphipods. *Estuarine and Coastal Marine Science, 11,* 593-604.

Eustace, R., Ritchie, H., Kilgallen, N., Piertney, S. B., & Jamieson, A. J. (2016). Morphological and ontogenetic stratification of abyssal and Hadal Eurythenes gryllus sensu lato (Amphipoda: Lysianassoidea) from the Peru-chile trench. *Deep Sea Research*, *109*, 91–98.

Evanno, G., Regnaut, S., & Goudet, J. (2005). Detecting the number of clusters of individuals using the software STRUCTURE: a simulation study. *Molecular Ecology*, *14*(8), 2611–2620.

France, S. C. (1993). Geographic variation among three isolated population of the hadal amphipod Hirondellea gigas (Crustacea: Amphipoda: Lysianassoidea). *Marine Ecology-Progress Series*, *92*, 277–287.

Fujii, T., Kilgallen, N., Rowden, A., & Jamieson, A. J. (2013). Deep-sea amphipod community structure across abyssal to hadal depths in the Peru-Chile and Kermadec trenches. *Marine Ecology. Progress*, *492*, 125–138.

Havermans, C., Sonet, G., D'Acoz, C., Nagy, Z., Martin, P., Brix, S., Held, C. (2013). Genetic and morphological divergences in the cosmopolitan deep-sea amphipod Eurythenes gryllus reveal a diverse abyss and a bipolar species. *PLoS*. doi.org/dx.doi.org/10.1371/journal.pone.0074218

Havermans, C. (2016). Have we so far only seen the tip of the iceberg? Exploring species diversity and distribution of the giant amphipod *Eurythenes*. *Biodiversity,* doi:10.1080/14888386.2016.1172257

Hofreiter, M., Serre, D., Poinar, H., Kuch, M., & Pääbo, S. (2001). Ancient DNA. *Nature Reviews Genetics*, *2*, 353–359.

Jakobsson, M., & Rosenberg, N. (2007). CLUMPP: a cluster matching and permutation program for dealing with label switching and multimodality in analysis of population structure. *Bioinformatics*, *23*(14), 1801–1806.

Jamieson, A. (2015). *The Hadal Zone: Life in the Deepest Oceans*. Cambridge University Press.

Jamieson, A., Fujii, T., Mayor, D., Solan, M., & Priede, I. G. (2010). Hadal trenches: the ecology of the deepest places on Earth. *Trends in Ecology & Evolution*, *25*(3), 190–197.

Jamieson, A., Fujii, T., & Solan, M. (2009). Liparid and macrourid fishes of the hadal zone: in situ observations of activity and feeding behaviour. *Proceedings of the Royal Society B.*, *276*(1659), 1037–1045.

Jamieson, A. J., Solan, M., & Fujii, T. (2009). Imaging deep-sea life beyond the abyssal zone. *Technology*, *50*(3), 41–46.

Jombart, T. (2008). adegenet: a R package for the multivariate analysis of genetic markers. *Bioinformatics*, *24*(11), 1403–1405.

462 Jombart, T., Devillard, S., & Balloux, F. (2010). Discriminant analysis of principal components:
463 a new method for the analysis of genetically structured populations. *BMC Genetics*,
464 *11*(94), 1–15.

465 Karig, D. (1970a). Kermadec arc-New Zealand tectonic confluence. *New Zealand Journal of*
466 *Geology and Geophysics*, *13*(1), 21–29.

467 Karig, D. (1970b). Ridges and basins of the Tonga-Kermadec Island arc system. *Journal of*
468 *Geophysical Research*, *75*(2), 239–254.

469 Kawabe, M., & Fujio, S. (2010). Pacific Ocean circulation based on observation. *Journal of*
470 *Oceanography*, *66*, 389–403.

471 Kawabe, M., Fujio, S., & Yanagimoto, D. (2003). Deep-water circulation at low latitudes in
472 the western North Pacific. *Deep Sea Research Part I: Oceanographic Research Papers*,
473 *50*(5), 631–656.

474 Keenan, K., McGinnity, P., Cross, T., Crozier, W. W., & Prodöhl, P. A. (2013). diveRsity: An R
475 package for the estimation and exploration of population genetics parameters and
476 their associated errors. *Methods in Ecology*, *4*(8), 782–788.

477 Kilgallen, N. (2015). Three new species of Hirondellea (Crustacea, Amphipoda,
478 Hirondelleidae) from hadal depths of the Peru-Chile Trench. *Marine Biology Research*,
479 *11*(1), 34–48.

480 Lacey, N., Rowden, A., Clark, M., Kilgallen, N., Linley, T., Mayor, D., & Jamieson, A. (2016).
481 Community structure and diversity of scavenging amphipods from bathyal to hadal
482 depths in three South Pacific Trenches. *Deep Sea Research Part I: Oceanographic*
483 *Research Papers*, *111*, 121–137.

484 Latch, E.K., Dharmarajan, G., Glaubitz, J.C., 2006. Relative performance of Bayesian clustering
485 software for inferring population substructure and individual assignment at low levels of
486 population differentiation. Conservation 7, 295–302.

487 Mitsuzawa, K., & Holloway, G. (1998). Characteristics of deep currents along trenches in the
488 northwest Pacific. *Journal of Geophysical Research*, *103*(C6), 13085–13092.

489 Oosterhout, C. Van, Hutchinson, W., Wills, D. P. M., & Shipley, P. (2004). MICRO-CHECKER:
490 software for identifying and correcting genotyping errors in microsatellite data.
491 *Molecular Ecology Notes*, *4*(3), 535–538.

492 Peakall, R., & Smouse, P. (2006). GENALEX 6: genetic analysis in Excel. Population genetic
493 software for teaching and research. *Molecular Ecology Notes*, *6*(1), 288–295.

494 Pelletier, B., Calmant, S., & Pillet, R. (1998). Current tectonics of the Tonga-New Hebrides
495 region. *Earth and Planetary Science Letters*, *164*(1-2), 263–276.

Pritchard, J., Stephens, M., & Donnelly, P. (2000). Inference of population structure using multilocus genotype data. *Genetics*, *155*(2), 945–959.

Quattrini, A., Baums, I., Shank, T. M., Morrison, C. L., & Cordes, E. E. (2015). Testing the depth-differentiation hypothesis in a deepwater octocoral. *Proceedings of the Royal Society B.*, *282*(1807), 1–9. doi.org/10.1098/rspb.2015.0008

Raymond, M., & Rousset, F. (1995). GENEPOP (version 1.2): population genetics software for exact tests and ecumenicism. *Journal of Heredity*, *86*(3), 248–249.

Reid, J. (1986). On the total geostrophic circulation of the South Pacific Ocean: Flow patterns, tracers and transports. *Progress in Oceanography*, *16*(1), 1–61.

Rex, M., & Etter, R. (2010). *Deep-sea biodiversity: pattern and scale*. Harvard University Press.

Ritchie, H., Cousins, N., Cregeen, S., & Piertney, S. B. (2013). Population genetic structure of the abyssal grenadier (Coryphaenoides armatus) around the mid-Atlantic ridge. *Deep Sea Research Part II: Topical Studies in Oceanography*, *98*(Part B), 431–437.

Ritchie, H., Jamieson, A., & Piertney, S. (2015). Phylogenetic relationships among hadal amphipods of the Superfamily Lysianassoidea: Implications for taxonomy and biogeography. *Deep Sea Research Part I: Oceanographic Research Papers*, *105*, 119–131.

Ritchie, H., Jamieson, A., & Piertney, S. (2016). Isolation and Characterization of Microsatellite DNA Markers in the Deep-Sea Amphipod Paralicella tenuipes by Illumina MiSeq Sequencing. *Journal of Heredity*, *107*(4367-371).

Roemmich, D., & McCallister, T. (1989). Large scale circulation of the North Pacific Ocean. *Progress in Oceanography*, *22*(2), 171–204.

Rosenberg, N. (2004). DISTRUCT: a program for the graphical display of population structure. *Molecular Ecology Notes*, *4*(1), 137–138.

Rousset, F. (2008). genepop'007: a complete re-implementation of the genepop software for Windows and Linux. *Molecular Ecology Resources*, *8*(1), 103–108.

Ryman, N., Palm, S., André, C., Carvalho, G., Dahlgren, T. G., Jorde, P. E., Ruzzante, D. E. (2006). Power for detecting genetic divergence: differences between statistical methods and marker loci. *Molecular*, *15*(8), 2031–2045.

Schellart, W., Lister, G., & Jessell, M. (2002). Analogue modeling of arc and backarc deformation in the New Hebrides arc and North Fiji Basin. *Geology*, *30*(4), 311–314.

Shaffer, G., Salinas, S., Pizarro, O., Vega, A., & Hormazabal, S. (1995). Currents in the deep ocean off Chile (30°S). *Deep Sea Research*, *42*(4), 425–436.

530 Stern, R. (2002). Subduction zones. *Reviews of Geophysics*, *40*(4), 3–1–3–38.

531 Talley, L. (1993). Distribution and formation of North Pacific intermediate water. *Journal of*
532 *Physical Oceanography*, *23*(3), 517–537.

533 Thurston, M. (1979). Scavenging abyssal amphipods from the north-east Atlantic Ocean.
534 *Marine Biology*, *51*(1), 55–68.

535 Thurston, M., Petrillo, M., & Della Croce, N. (2002). Population structure of the
536 necrophagous amphipod Eurythenes gryllus (Amphipoda: Gammaridea) from the
537 Atacama Trench (south-east Pacific Ocean). *Journal of the Marine Biological Association*
538 *of the United Kingdom*, *82*(2), 205–211.

539 Wolff, T. (1959). The hadal community, an introduction. *Deep Sea Research and*
540 *Oceanographic Abstracts*, *6*, 95–124. doi.org/10.1016/0146-6313(59)90063-2

541 Wolff, T. (1970). The concept of the hadal or ultra-abyssal fauna. *Deep Sea Research and*
542 *Oceanographic Abstracts*, *17*(6), 983–1003.

Table 1. Sampling locations for seven populations of *Paralicella* across five trenches sampled in the Pacific Ocean.

Genetic Clade	Population	Trench	Depth (m)	Latitude	Longitude	Station
1	Kermadec	Kermadec	6007	26° 43.9'S	175° 11.3'W	SO197-1a
	Japan	Japan	6945	40° 15.3'N	144° 30.8'E	KH0703-1
	Mariana	Mariana	5469	18° 49.2'N	149° 50.6'E	KR0716-1
	Peru-Chile	Peru-Chile	5329	04° 27.0'S	81° 54.7'W	SO209-03
			6173	07° 48.0'S	81° 17.0'W	SO209-35
2	Kermadec	Kermadec	6007	26° 43.9'S	175° 11.3'W	SO197-1a
	Peru-Chile	Peru-Chile	5329	04° 27.0'S	81° 54.7'W	SO209-03
			6173	07° 48.0'S	81° 17.0'W	SO209-35
	New Hebrides	New Hebrides	2500	21° 13.2'S	168° 40.0'E	KAH1310-037
			4100	27° 44.8'S	174° 15.0'E	KAH1310-039

Table 2. Genetic diversity statistics for seven *a priori* populations of *Paralicella* spp. across 16 microsatellite loci; population size (n), effective number of alleles (n_e), allelic richness (a_r), and observed heterozygosity (H_O).

Genetic Clade	Population	*n*	n_e	a_r	$H_O \pm SD$
1	Kermadec	4	2.81	1.81	0.18 ± 0.07
	Japan	24	6.44	3.47	0.38 ± 0.04
	Mariana	24	6.56	3.44	0.34 ± 0.03
	Peru-Chile	15	5.38	3.11	0.32 ± 0.03
2	Kermadec	26	5.63	3.68	0.22 ± 0.05
	Peru-Chile	2	2.75	0.66	0.03 ± 0.03
	New Hebrides	14	4.13	2.55	0.22 ± 0.05

Table 3. Wright's F_{ST} pairwise estimates of population genetic differentiation among seven *a priori* *Paralicella* spp. populations based on 16 microsatellite loci. F_{ST} estimates denoted with a single asterisk are significant at the 5% level and those denoted with two asterisks are significant at the 1% level.

Genetic Clade		1				2		
	Populations	Kermadec	Japan	Mariana	Peru-Chile	Kermadec	Peru-Chile	New Hebrides
1	Kermadec	-						
	Japan	N/A	-					
	Mariana	N/A	0.02**	-				
	Peru-Chile	N/A	0.05**	0.05**	-			
2	Kermadec	N/A	0.33**	0.32**	0.23**	-		
	Peru-Chile	N/A	N/A	N/A	N/A	N/A	-	
	New Hebrides	N/A	0.30**	0.29**	0.21**	0.16**	N/A	-

Table 4. Analysis of molecular variance (AMOVA) partitioning of genetic variance between species, between populations within species, and among individuals within populations.

Source of Variation	d.f.	Sum of Squares	Variance	Total (%)
Between Species	1	175.36	1.47	21
Between Populations	5	85.95	0.46	7
Within Populations	211	1027.83	4.87	72
Total	217	1288.83	6.79	100

Table 5. The number of immigrants per generation (ΘM) between populations of *Paralicella* estimated using Migrate-n based upon 16 microsatellite loci.

Genetic Clade			1				2		
			MIGRATION TO						
		Populations	Kermadec	Japan	Mariana	Peru-Chile	Kermadec	Peru-Chile	New Hebrides
1	MIGRATION FROM	Kermadec	-	0	781	422			
		Japan	0	-	898	503			
		Mariana	116	781	-	512			
		Peru-Chile	153	871	718	-			
2		Kermadec					-	0	0
		Peru-Chile					153	-	0
		New Hebrides					0	0	-

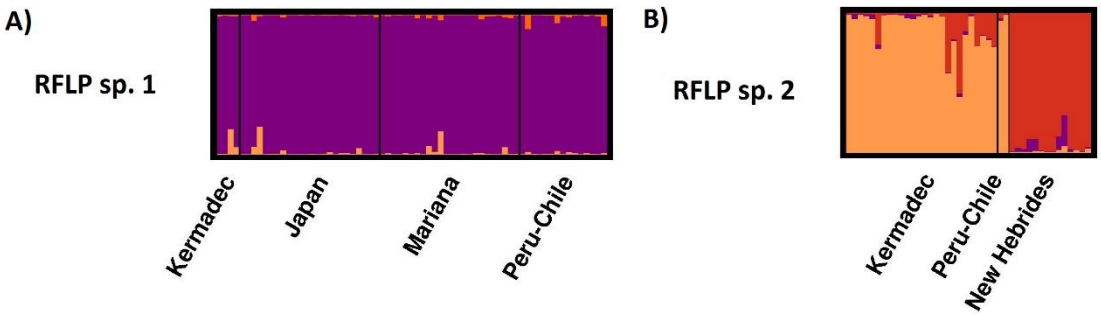

Figure 1. Structure output showing individual membership coefficients derived from Bayesian inferences of genetic structure across populations of A) RFLP sp. 1 and B) RFLP sp. 2, for K=3, where each individual is represented by a vertical column. Coefficients are averaged across replicate runs using the standard admixture model without including sampling locations as prior information (non-LOCPRIOR).

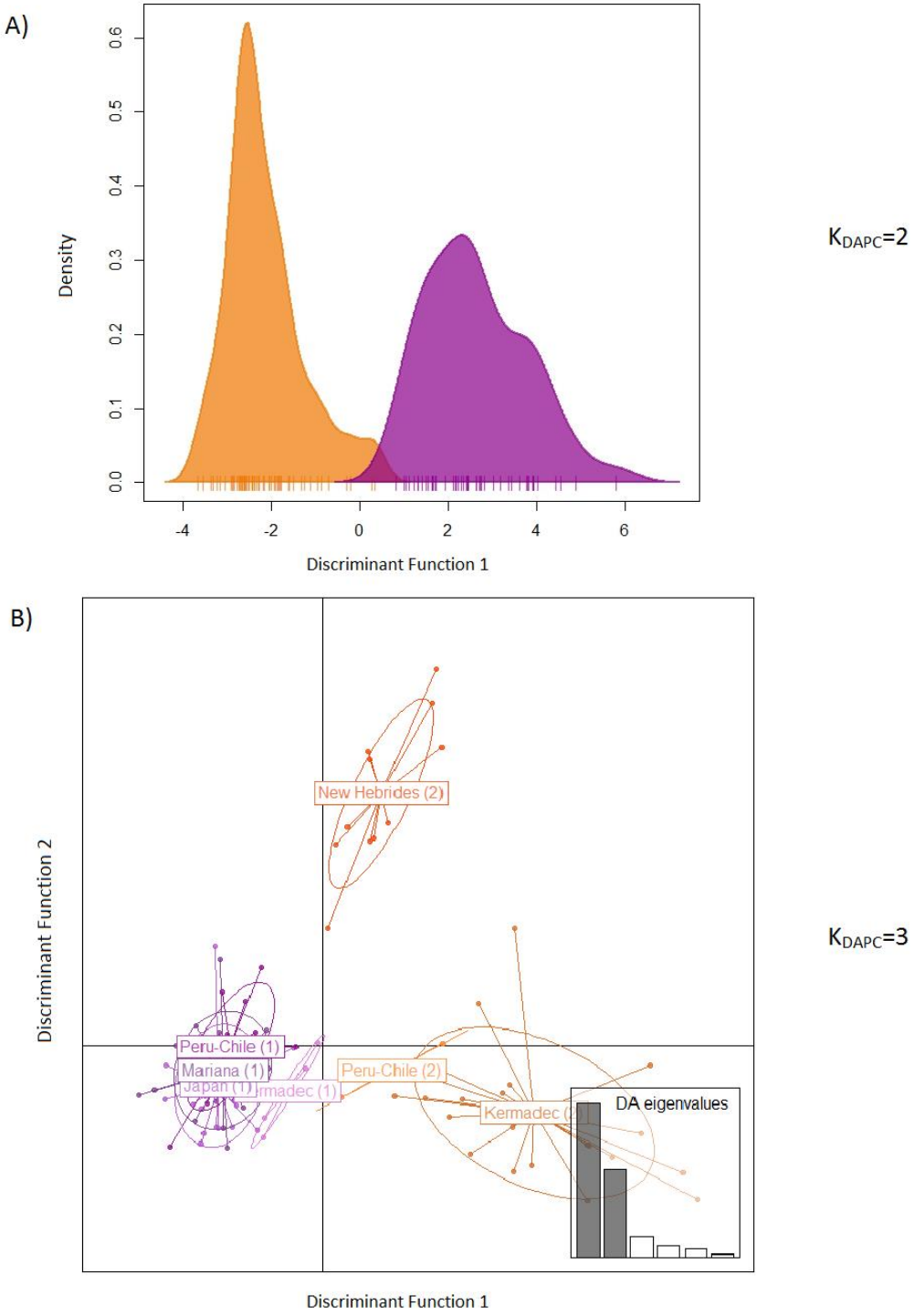

Figure 2. Summary of discriminant analysis of principal components (DAPC) across the seven pre-defined *Paralicella* spp. populations: (A) Distribution plot of K_{DAPC}=2 for the two RFLP species. (B) Ordination plot of K_{DAPC}=3 for the seven genetic clusters. Genetic clusters are split into the two RFLP species by colour (RFLP species 1 in purple and RFLP species 2 in orange) and pre-defined populations are labelled. The bottom right inset shows the eigenvalues of the principal components in relative magnitude.

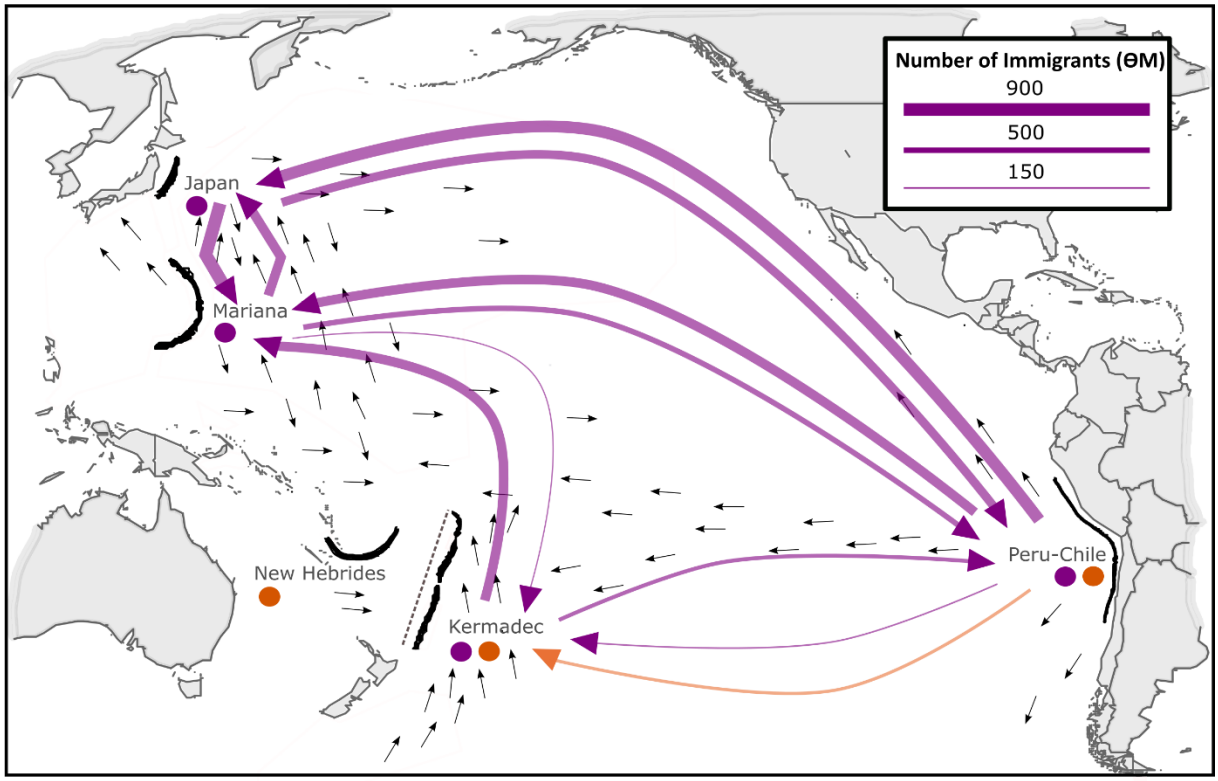

Figure 3. Map of the Pacific Ocean showing locations of the five hadal trenches. Coloured circles indicate the presence of Clade 1 (purple) or Clade 2 (orange) individuals. Bold coloured arrows indicate direction of migration as calculated by MIGRATE-N and divMigrate and are scaled to indicate the number of immigrants per generation (ΘM) where purple arrows show migration patterns between Clade 1 populations and orange arrows show migration patterns between Clade 2 populations. The black dotted line represents the position of the Kermadec-Tonga forearc. Small black arrows indicate direction of seafloor currents compiled from data in Reid (1986;1997), Roemmich and McCallister (1989) and Talley (1993).

Supplemental Table 1. Comparison of connectivity models in Migrate-n using the Bezier approximate log marginal likelihoods (Bezier lmL) and the log Bayes factor (LBF).

	Model	Bezier lmL	LBF	Rank
RFLP sp. 1	Full	-652172.17	-463743.31	3
	Current	**-188428.86**	**0**	**1**
	Counter-current	-191951.73	-3522.87	2
RFLP sp. 2	**Full**	**-67430.78**	**0**	**1**
	Current	-75407.39	-7976.61	2
	Counter-current	-175133.82	-107703.04	3